CC-NORD: A Camera-Invariant Global Color Constancy Dataset

Diclehan Ulucan, Oguzhan Ulucan, Marc Ebner
Institut für Mathematik und Informatik, Universität Greifswald, Greifswald, Germany
{diclehan.karakaya, oguzhan.ulucan, marc.ebner}@uni-greifswald.de

***Abstract*—Color constancy benchmarks are mostly created by using cameras with similar hardware and by capturing the scenes under similar illuminants. Therefore, ground truth information is affected by the cameras' sensor response characteristics, and during the evaluation of color constancy algorithms, some illuminants are neglected. In this study, we introduce a large-scale synthetic color constancy dataset called *CC-NORD*. Since CC-NORD is formed by using computer graphics, the ground truth information is independent of the capturing device. Also, to provide images created under a wide range of illuminants, the scenes in CC-NORD are rendered with a high number of distinct illuminants including lights having values away from the color temperature curve. To the best of our knowledge, this is the first color constancy dataset containing scenes rendered under illuminants on the edge and outside the color temperature curve. Upon publication, CC-NORD will be publicly available on the first author's webpage.**

***Index Terms*—Computational color constancy, dataset**

I. Introduction

Perceiving the colors of objects regardless of the illumination conditions is a strong attribute of the human visual system and it is called *color constancy* [1]. Even though perceived colors are not physical properties of objects but products of the brain, they are associated with objects and they provide important features for both human and machine vision systems [2]. While the human visual system unconsciously *discounts the illumination* to perceive the actual reflectance of the scene, computer vision systems have difficulty in estimating the reflectance values of objects. This difficulty arises from the nature of image formation since a digital image is a measured signal, which is obtained by the integration of the surface reflectance, light source, and camera sensor functions as follows;

$$I_j(x,y) = \int R(x,y,\lambda)L(x,y,\lambda)S_j(\lambda)d\lambda \qquad (1)$$

where, $I_j(x,y)$ is an image, (x,y) represents the spatial location of a pixel, subscript j represents the corresponding color channel of the image (red, green and blue), $R(x,y,\lambda)$ is the surface reflectance, $L(x,y,\lambda)$ is the illumination, and $S_j(\lambda)$ is the sensitivity of the camera's color sensor.

As seen from Eqn. 1, the colors of the scene are prone to be shifted in the direction of the light source and affected by the capturing device specifications. Without filtering out the illumination, it is impossible to obtain the actual reflectance values of the objects. The field trying to solve this ill-posed problem by finding new and efficient ways to discount the illumination from a scene is called computational color constancy. Due to the importance it holds, it is well studied and many color constancy algorithms have been introduced in the past decades. In general, color constancy methods can be grouped into three main categories; traditional-based, learning-based, and data-driven methods. While traditional algorithms make assumptions based on the statistical properties of images [3], [4], [5], [6], [7], [8], [9], [10], [11], [12], [13], [14], data-driven and learning-based approaches estimate the illuminant by extracting information and learning from samples present in their large-scale training sets [15], [16], [17].

Apart from numerous algorithms, also several datasets have been introduced in the field of color constancy. One of the largest benchmarks is INTEL-TAU formed by Lakoom *et. al* [18]. It contains a total of 7022 images captured with 3 different camera models, Canon 5DSLR and Nikon D810 DSLR, and Mobile Sony IMX135. In order to prevent multi-illumination conditions, images are obtained with one dominant light source illuminating the scene. Moreover, the dataset is organized to mask all the sensitive information to obey the General Data Protection Regulation act [19]. Since it contains a large number of high-resolution images, INTEL-TAU is suitable for learning-based color constancy studies. The well-known RECommended ColorChecker dataset [20] is a modified version of the Gehler-Shi color constancy dataset [21]. RECommended ColorChecker contains 568 indoor and outdoor images captured with two camera models, Canon 1D and Canon 5D, and to avoid multi-illuminant conditions the images are captured under one dominant light source. Since the dataset contains distinct types of indoor and outdoor scenes, it is valuable for color constancy studies. However, the number of images is not sufficient for learning-based color constancy methods. The NUS-8 dataset is another publicly available dataset introduced by Cheng *et. al* [8]. While generating the dataset, 9 different camera models are used to capture a total of 1853 images. The Cube++ dataset [22] is the extension of the Cube dataset [23] and it contains 1698 indoor and outdoor images. The images are captured with a Canon EOS 550D camera. The images contain one dominant illuminant illuminating the scene, which makes the dataset useful for color constancy studies aiming at estimating the global illuminant. The statistical distribution of the light source in Cube++ is similar to the NUS-8 dataset. The SFU HDR dataset introduced by Funt *et. al* [24], [25] is another well-

known color constancy benchmark. This dataset contains 105 high dynamic range images which are captured using a Nikon D700 camera. The global illumination of the scene is found from the color charts placed at diverse locations in the scene. A recent color constancy dataset, The Rendered WB dataset, is created by Afifi *et. al* [17]. This dataset is one of the largest benchmarks containing 65416 sRGB images and corresponding ground-truth information. The images are rendered under different white-balance settings with diverse camera picture styles. Moreover, 2881 of the images are obtained from four different mobile phones and one DSLR camera, which makes this dataset also useful for color constancy studies related to mobile applications. Since the dataset is large, it is useful for learning-based and data-driven methods.

One of the common drawbacks of these datasets is the fact that the scenes are captured under similar lighting conditions. As explicitly shown in our recent study [12], the limitation in the variety of illuminants is a critical drawback, especially for learning-based methods, which expect their training and test sets to be somehow similar. In real-life applications, these algorithms may face images with different statistical distributions and their performance might decrease significantly. Also, in the study of Buzzelli *et al.*, where the shortcomings of color constancy datasets are analyzed in detail, it is reported that there is a lack of images illuminated by artificial lights in existing benchmarks [26]. Another shortcoming of the datasets is the usage of similar hardware while capturing the images [26], [27]. Gao *et al.* stated that in existing color constancy benchmarks the ground truth is extracted from a particular region of an image, which is captured by the camera sensors, hence naturally the ground truth is dependent on the camera specifications, i.e. the ground truth is not entirely accurate due to the effect of the capturing device [27]. A similar discussion on the device dependency of ground truths is discussed in the recent study of Buzzelli *et al.*, where it is stated that the camera specifications affect the acquired ground truths [26]. Furthermore, as pointed out in our recent study and the work of Qian *et al.*, since several color constancy methods use the camera spectral sensitivity as prior information, and the hardware specifications affect the statistical distribution of images, an inevitable bias is present in data-dependent algorithms [10], [12]. These statements underline the need and importance of a camera-invariant color constancy dataset containing different illumination conditions.

Based on these observations, in this study, we created a large-scale color constancy dataset, namely *CC-NORD*, by using computer graphics. In CC-NORD, ground truth information independent of any hardware specifications is provided, i.e. actual canonical images are created. Moreover, each scene is rendered with 18 different illuminants, which are changed for each scene, and with 7 lights located at the beginning and end and also away from the color temperature curve (CTC). The importance of considering these lights in color constancy studies has been reported in our recent study [12] by showing that data-dependent color constancy methods face an inevitable challenge when they need to white-balance images captured under out of ordinary lights. The aim of providing CC-NORD is to enable researchers in this field to have access to camera-invariant ground truth information and images that contain a high number of distinct illuminants. We demonstrate the usability of CC-NORD by benchmarking 13 different color constancy methods.

Our contributions can be summarized as follows:

- We created a large-scale camera-invariant color constancy dataset that includes lights located at the beginning and end and also away from the CTC. To the best of our knowledge, this is the first color constancy benchmark that considers these illuminants.
- We created the largest synthetic global color constancy benchmark considering lights beyond the CTC and provide 10000 images with actual ground truth information independent of any hardware specification.

This paper is organized as follows. Section II presents the formation of the dataset. Section III gives the experimental results of color constancy methods used to evaluate the usability of the dataset. Section IV gives a brief summary of the study.

II. The Dataset

In color constancy, obtaining camera-invariant ground truth information is troublesome. In most studies, a color checker is used to find the RGB values of the light source in the scene which causes an error in the ground truth illumination as aforementioned. Moreover, in most color constancy datasets, images captured under similar illumination conditions are present. Thereupon, we formed CC-NORD by using computer graphics to provide actual ground truth information independent of camera specifications and to render scenes under various lights. The images in CC-NORD are created through an algorithm designed in the open-source 3D graphics toolkit called OpenSceneGraph (www.openscenegraph.com), by following a similar strategy we used for our recent intrinsic images dataset called IID-NORD [28]. Textures are both synthetically generated and taken from Pixabay (pixabay.com). It is worth mentioning here that in CC-NORD, there is no sensitive information that has to be masked out and no need to perform black-level calibration. Also, no color checker is present in the scenes. Hence, CC-NORD can be easily used without making any adjustments to the images.

In total 10000 scenes with a resolution of 1400×965 pixels are rendered (Fig. 1). All images have a linear response function. There are two different setups in CC-NORD; *(i)* close-up shootings, and *(ii)* indoor scenes. These setups are preferred since it is known that estimating the illuminant of close-up shootings and indoor scenes is more difficult [26]. The objects are randomly placed and the viewing angle is changed to increase the variety of scenes in the dataset. Furthermore, since noise is commonly observed in real photographs, zero-mean, Gaussian white noise with variances of 10^{-4} and 2×10^{-4} is randomly added to some of the images.

The scenes in CC-NORD contain various 3D models. In each consecutive render, at least one asset is replaced by another to increase the variety in the rendered images.

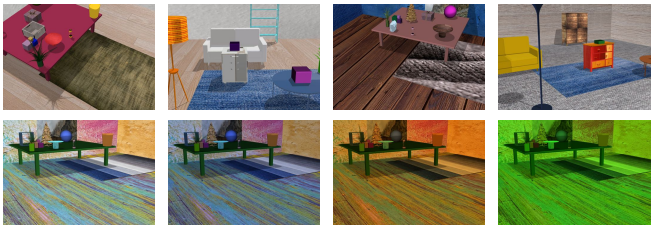

Fig. 1: Examples from CC-NORD. (Top row) Different scenes and (bottom row) a scene rendered under different illuminants.

The textures of the objects are chosen individually. Textures with uniform and non-uniform color distribution, sharp color changes, and different motifs and patterns are applied to the assets. These different texture characteristics are considered since all of them are commonly observable in our daily lives, i.e. they are simple representations of textures captured in real-life with cameras. Furthermore, by using various types of textures it is aimed to prevent any bias in learning-based color constancy models arising due to the uniformity of data.

In each scene, a single point light source is positioned randomly. Point light sources are preferred rather than directional light to obtain dynamic shadow casts and a better indoor illumination effect. Each scene is rendered with 25 illuminants, where 7 of them are lights from the beginning and end and also away from the color temperature curve, and 18 of them are illuminants commonly observed in real photographs (Fig. 1). These widely used illuminants are determined by analyzing three of the most frequently used benchmarks in this field. First of all, the illuminants of the INTEL-TAU [16], RECommended ColorChecker [20], and Cube+ [23] datasets are collected and repetitive illuminants are removed. Then, the remaining illuminants that have unique RGB triplets are given to a k-means clustering algorithm. k is set to 18 because the data can be grouped relatively uniform and each cluster's statistical distribution has a reasonable variance using this value of k. Afterwards, every scene is rendered by choosing one illuminant from each cluster. Hence, a high number of different illuminants is included in CC-NORD. Subsequently, each scene is also rendered with 7 lights having a corresponding value from either the beginning or end or away from the color temperature curve. These lights are used in various applications, yet in particular, the lights away from the CTC are not present in existing color constancy datasets [12]. In our recent study [12] we reported that the absence of these lights in existing color constancy datasets causes a bias in data-dependent color constancy methods, i.e. they fail to discount these illuminants. This shortcoming may cause problems in computer vision pipelines, where learning-based and data-driven color constancy methods are used in the pre-processing step.

The dynamic soft shadows in CC-NORD are created using the Parallel Split Shadow Maps (PSSM) technique [29]. PSSM uses the planes, which are parallel to the view plane in order to split the view frustum into several pieces. Afterwards, it creates multiple small shadow maps for these pieces. Hence, PSSM takes into account the observation that distinct shadow map sampling densities are required for points, which are located at a different distance to the viewpoint. Since it allows proper rendering of dynamic shadows and produces a relatively low aliasing effect PSSM is preferred in CC-NORD.

III. Experiments and Discussion

The usability of CC-NORD is demonstrated by using the following traditional-based color constancy methods; gray world (GW) [3], shades of gray (SoG) [4], 1^{st} and 2^{nd} order gray-edge (GE) [5], weighted gray-edge (WGE) [6], double-opponent cells based color constancy (DOCC) [7], PCA based color constancy (PCA-CC) [8], color constancy with local surface reflectance estimation (LSRS) [9], mean-shifted gray pixels (MSGP) [10], gray pixels (GI) [11], and block-based color constancy (BB-CC) [12], and learning-based methods; C5 [15], and C3AE [16] (Table I). The methods are used in their default settings without any modification. Also, in order to show the importance of out-of-ordinary lights, learning-based methods trained on standard benchmarks are tested on CC-NORD directly. The experiments are performed on an Intel i7 CPU @ 2.7 GHz Quad-Core 16 GB RAM machine.

In order to test the algorithms on CC-NORD, two statistical evaluation methods are used. Firstly, the well-known angular error metric [30], which is defined as the angle between the actual RGB values of the global light and the estimated light is used. Secondly, the ΔE 2000 [31], [32] metric, which investigates the color difference of images is used to evaluate the algorithms. ΔE scores less than 1 are imperceptible, while a score in the range $[1, 4)$ might also be unnoticeable for an observer [2], [33]. The mean of the best 25% (B.25%), the mean of the worst 25% (W.25%), the median (med.), and the mean of the angular error and ΔE are reported in Table I.

As it can be deduced from B.25% of the angular error scores, CC-NORD allows color constancy algorithms to successfully estimate the illuminant. Especially, when the best white-balanced images are considered traditional color constancy methods reach very low angular errors. However, as it can be seen in the outcomes of the W.25% of the angular error, CC-NORD challenges the algorithms. In particular, the performance of the learning-based methods is severely affected by the illuminants, which are not present in their training sets. It is clear that unless images with distinct illuminants are added to their training sets, data-dependent algorithms will perform poorly when they face such lights.

The mean ΔE scores of several traditional color constancy methods are around 4, hence images white-balanced with the illuminant estimates of these algorithms are visually very similar to the ground truth image. On the other hand, the ΔE results of the learning-based color algorithms show that there is a significant perceivable color difference between the white-balanced image and the ground truth. All these observations also coincide with the visual results of the algorithms (Fig. 2).

In Fig. 2, the visual outcomes of several traditional algorithms are provided together with the results of C3AE, which

TABLE I: Statistical analysis of the algorithms. For each metric, the best result is highlighted. The last column contains the average run time in seconds.

	Angular Error				ΔE 2000				
Algorithms	**Mean**	**Med.**	**B.25%**	**W.25%**	**Mean**	**Med.**	**B.25%**	**W.25%**	**Run time**
GW	6.831	5.517	1.242	15.124	6.376	5.569	1.829	12.356	0.125
SoG	4.843	3.889	0.537	10.857	4.881	4.034	0.748	10.658	0.189
1^{st} order GE	5.159	4.231	1.396	**10.425**	5.433	4.657	1.827	10.362	0.313
2^{nd} order GE	4.656	3.433	0.893	10.502	4.803	3.689	1.170	10.015	0.345
WGE	4.737	2.275	0.452	13.547	4.608	2.584	0.557	11.918	2.039
MSGP	4.123	**1.269**	0.295	11.939	**3.750**	**1.455**	0.464	10.519	0.516
GI	**4.032**	1.293	**0.183**	12.030	3.851	1.487	**0.322**	11.116	0.340
LSRS	4.567	3.567	0.577	10.495	4.248	3.819	0.952	**8.398**	0.114
DOCC	5.796	2.070	0.320	15.874	7.200	2.600	0.458	20.031	0.325
PCA-CC	7.401	4.860	0.306	18.057	7.591	5.132	0.510	18.081	0.157
BB-CC	4.548	3.322	0.676	10.606	4.263	3.837	1.012	8.470	0.231
C5	19.848	16.018	7.309	38.887	15.760	13.922	7.053	27.790	0.086
C3AE	12.186	10.240	4.830	22.937	11.959	10.489	4.719	21.902	**0.037**

is a learning-based method. All algorithms perform well for the two input images given in the first and third rows, which are illuminated by illuminants that are commonly observed in color constancy benchmarks. However, when the scene is illuminated by a light beyond the standard illuminants, it can be seen that C3AE faces a challenge in estimating the illuminant. The reasons behind the performance decay of learning-based color constancy methods are their dependency on camera sensor characteristics and bias in their training data [12], [27]. These methods are inevitably challenged when they face images with different statistical distributions that are not present in their training sets. Thus, CC-NORD can be included into the training sets of learning-based algorithms to decrease the bias in the data. As a final note, we did not train the learning-based models on CC-NORD, since our aim is to show the importance of considering images with different statistical distributions and to demonstrate the problems related to the usage of similar data in learning-based methods.

IV. Conclusion

Color constancy algorithms are benchmarked on datasets, which are created using capturing devices having similar hardware specifics. Furthermore, most datasets contain similar illuminants, thus color constancy methods are neither trained nor tested on a wide variety of illuminants which limits the effectiveness in particular of learning-based color constancy algorithms. Thereupon, in this study, we created a synthetic color constancy benchmark. CC-NORD satisfies the needs of existing datasets, i.e. diverse illuminants and camera-invariant ground truths, while it also challenges color constancy algorithms since it includes indoor close-up shootings and out-of-ordinary lights. In the experimental results, we have shown the importance of considering different types of illuminants and using data created independent of hardware characteristics. CC-NORD can help to reduce the bias in learning-based and data-driven algorithms. CC-NORD can be either used alone or combined with a dataset containing real scenes to train and test learning-based methods.

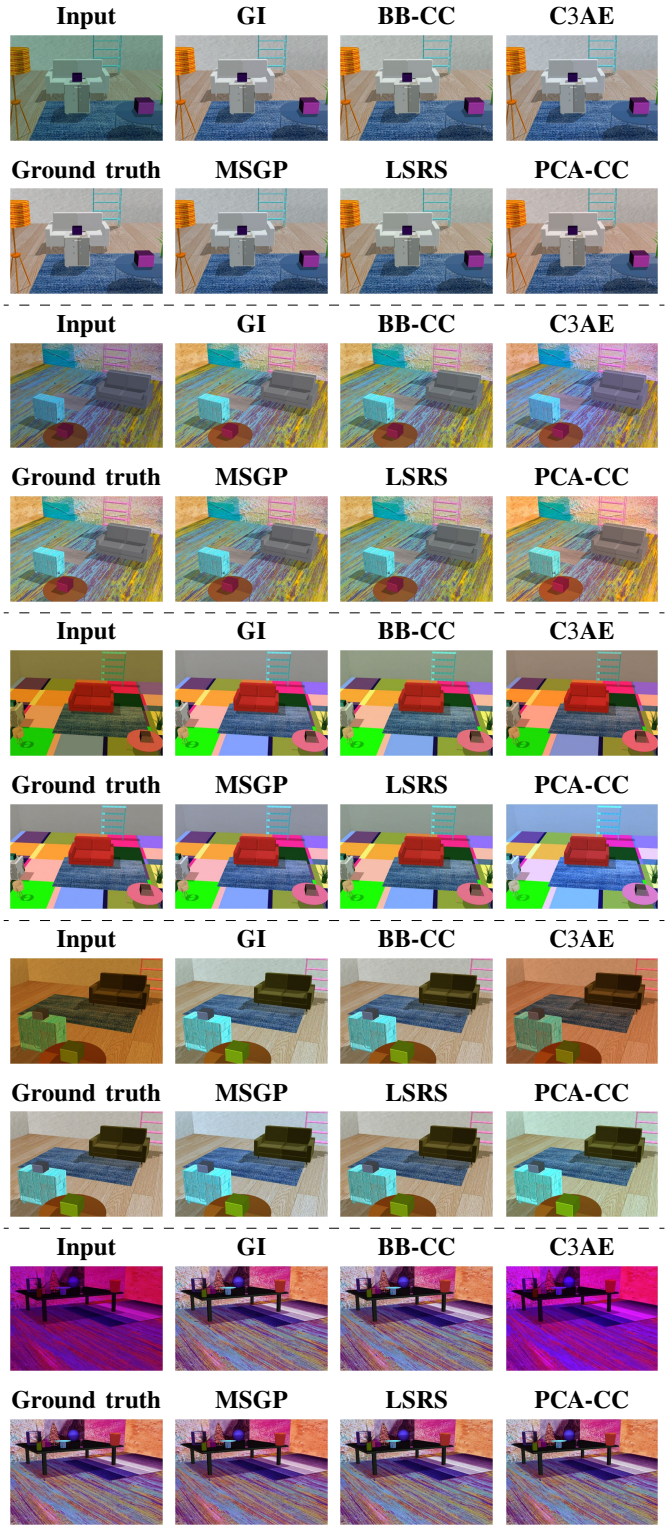

Fig. 2: Visual comparison of the algorithms.

References

[1] M. Ebner and J. Hansen, "Depth map color constancy," *Bio-Algorithms Med-Syst.*, vol. 9, no. 4, pp. 167–177, 2013.

[2] M. Ebner, *Color Constancy, 1st ed.*, Wiley Publishing, 2007.

[3] G. Buchsbaum, "A spatial processor model for object colour perception," *J. Franklin Inst.*, vol. 310, pp. 1–26, 1980.

[4] G. D. Finlayson and E. Trezzi, "Shades of gray and colour constancy," in *Color and Imag. Conf.*, Scottsdale, AZ, USA, 2004, Society for Imaging Science and Technology, pp. 37–41.

[5] J. Van De Weijer, T. Gevers, and A. Gijsenij, "Edge-based color constancy," *IEEE Trans. Image Process.*, vol. 16, pp. 2207–2214, 2007.

[6] A. Gijsenij, T. Gevers, and J. Van De Weijer, "Physics-based edge evaluation for improved color constancy," in *Conf. Comput. Vision Pattern Recognit.*, Miami, FL, USA, 2009, IEEE, pp. 581–588.

[7] S. Gao, K. Yang, C. Li, and Y. Li, "Color constancy using double-opponency," *IEEE Trans. Pattern Anal. Mach. Intell.*, vol. 37, pp. 1973–1985, 2015.

[8] D. Cheng, D. K. Prasad, and M. S. Brown, "Illuminant estimation for color constancy: Why spatial-domain methods work and the role of the color distribution," *J. Opt. Soc. America A*, vol. 31, pp. 1049–1058, 2014.

[9] S. Gao, W. Han, K. Yang, C. Li, and Y. Li, "Efficient color constancy with local surface reflectance statistics," in *Eur. Conf. Comput. Vision*, Zurich, Switzerland, 2014, Springer, pp. 158–173.

[10] Y. Qian, S. Pertuz, J. Nikkanen, J.-K Kämäräinen, and J. Matas, "Revisiting gray pixel for statistical illumination estimation," *arXiv preprint arXiv:1803.08326*, 2018.

[11] Y. Qian, J.-K. Kamarainen, J. Nikkanen, and J. Matas, "On finding gray pixels," in *Conf. Comput. Vision Pattern Recognit.*, Long Beach, CA, USA, 2019, IEEE/CVF, pp. 8062–8070.

[12] O. Ulucan, D. Ulucan, and M. Ebner, "Color constancy beyond standard illuminants," in *Int. Conf. Image Process.*, Bordeaux, France, 2022, IEEE, pp. 2826–2830.

[13] O. Ulucan, D. Ulucan, and M. Ebner, "BIO-CC: Biologically inspired color constancy," in *Brit. Mach. Vision Conf.*, London, UK, 2022, BMVA Press.

[14] O. Ulucan, D. Ulucan, and M. Ebner, "Block-based color constancy: The deviation of salient pixels," in *Int. Conf. Acoust. Speech Signal Process.*, Rhodes Island, Greece, 2023, IEEE, pp. 1–5.

[15] M. Afifi, J. T. Barron, C. LeGendre, Y.-T. Tsai, and F. Bleibel, "Cross-camera convolutional color constancy," in *Int. Conf. Comput. Vision*, Montreal, QC, Canada, 2021, IEEE/CVF, pp. 1981–1990.

[16] F. Laakom, J. Raitoharju, A. Iosifidis, J. Nikkanen, and M. Gabbouj, "Color constancy convolutional autoencoder," in *Symp. Ser. Comput. Intell.*, Xiamen, China, 2019, IEEE, pp. 1085–1090.

[17] M. Afifi, B. Price, S. Cohen, and M. S. Brown, "When color constancy goes wrong: Correcting improperly white-balanced images," in *Conf. Comput. Vision Pattern Recognit.*, Long Beach, CA, USA, 2019, IEEE/CVF, pp. 1535–1544.

[18] F. Laakom, J. Raitoharju, J. Nikkanen, A. Iosifidis, and M. Gabbouj, "Intel-Tau: A color constancy dataset," *IEEE Access*, vol. 9, pp. 39560–39567, 2021.

[19] P. Voigt and A. Von dem Bussche, "The eu general data protection regulation (gdpr)," *A Practical Guide, 1st Ed., Cham: Springer International Publishing*, vol. 10, no. 3152676, pp. 10–5555, 2017.

[20] G. Hemrit, G. D. Finlayson, A. Gijsenij, P. Gehler, S. Bianco, B. Funt, M. Drew, and L. Shi, "Rehabilitating the colorchecker dataset for illuminant estimation," in *Color Imag. Conf.*, Vancouver, BC, Canada, 2018, Society for Imaging Science and Technology, pp. 350–353.

[21] P. V. Gehler, C. Rother, A. Blake, T. Minka, and T. Sharp, "Bayesian color constancy revisited," in *Conf. Comput. Vision Pattern Recognit.*, Anchorage, AK, USA, 2008, IEEE, pp. 1–8.

[22] E. Ershov, A. Savchik, I. Semenkov, N. Banić, A. Belokopytov, D. Senshina, K. Koščević, M. Subašić, and S. Lončarić, "The cube++ illumination estimation dataset," *IEEE Access*, vol. 8, pp. 227511–227527, 2020.

[23] N. Banić, K. Koščević, and S. Lončarić, "Unsupervised learning for color constancy," *arXiv preprint arXiv:1712.00436*, 2017.

[24] B. Funt and L. Shi, "The effect of exposure on maxrgb color constancy," in *Human Vision Electron. Imag. XV*, San Jose, CA, United States, 2010, SPIE, vol. 7527, pp. 282–288.

[25] B. Funt and L. Shi, "The rehabilitation of maxrgb," in *Color Imag. Conf.*, San Antonio, TX, USA, 2010, Society for Imaging Science and Technology, vol. 2010, pp. 256–259.

[26] M. Buzzelli, S. Zini, S. Bianco, G. Ciocca, R. Schettini, and M. K. Tchobanou, "Analysis of biases in automatic white balance datasets and methods," *Color Res. Appl.*, vol. 48, no. 1, pp. 40–62, 2023.

[27] S. Gao, M. Zhang, C. Li, and Y. Li, "Improving color constancy by discounting the variation of camera spectral sensitivity," *J. Opt. Soc. America A*, vol. 34, no. 8, pp. 1448–1462, 2017.

[28] D. Ulucan, O. Ulucan, and M. Ebner, "IID-NORD: A comprehensive intrinsic image decomposition dataset," in *Int. Conf. Image Process.)*, Bordeaux, France, 2022, IEEE, pp. 2831–2835.

[29] F. Zhang, H. Sun, L. Xu, and L. K. Lun, "Parallel-split shadow maps for large-scale virtual environments," in *Int. Conf. Virtual Reality Continuum Appl.*, Hong Kong, China, 2006, ACM, pp. 311–318.

[30] S. D. Hordley and G. D. Finlayson, "Re-evaluating colour constancy algorithms," in *IEEE Int. Conf. Pattern Recognit.*, Cambridge, UK, 2004, IEEE, vol. 1, pp. 76–79.

[31] M. R. Luo, G. Cui, and B. Rigg, "The development of the CIE 2000 colour-difference formula: CIEDE2000," *Color Res. Appl.*, vol. 26, no. 5, pp. 340–350, 2001.

[32] G. Sharma, W. Wu, and E. N. Dalal, "The CIEDE2000 color-difference formula: Implementation notes, supplementary test data, and mathematical observations," *Color Res. Appl.*, vol. 30, no. 1, pp. 21–30, 2005.

[33] D. Ulucan, O. Ulucan, and M. Ebner, "Intrinsic image decomposition: Challenges and new perspectives," in *Int. Conf. Image Process. Vision Eng.*, Prague, Czech Republic, 2023, INSTICC, pp. 57–64.